Band offsets for strained $In_xGa_{1-x}As/Al_yGa_{1-y}As$ heterointerfaces

D. J. Arent
IBM Research Division, Zurich Research Laboratory, Säumerstrasse 4, CH-8803 Rüschlikon, Switzerland
(Received 20 November 1989)

Valence-band offsets for pseudomorphically strained $In_xGa_{1-x}As/Al_yGa_{1-y}As$ ternary-on-ternary heterointerfaces have been calculated as a function of both indium and aluminum content. The unstrained valence-band offsets were considered within the virtual-crystal approximation, accounting for band parabolicity and alloy mixing. Strain was introduced as a perturbation with composition-dependent material parameters, and is shown to strongly influence the valence-band offsets. Equivalent conduction-band-offset ratios are shown to be nonconstant and extremely variable as a function of both In and Al content and are compared to recent experimental data. Various formalisms to calculate the partitioning coefficient for hydrostatic band-gap deformation are presented and discussed, and our analysis indicates that a significant portion of the band-gap variation induced by hydrostatic strain resides in the valence band. Investigation of the spin-split light-hole band level under strain indicates that both type-I and type-II heterointerfaces are achievable with an appropriate choice of compositions.

I. INTRODUCTION

The nature of band-edge discontinuities—commonly called band offsets—are of vital interest for a comprehensive understanding of heterointerfaces of semiconductor materials. For the ever-expanding field of III-V heterostructures, optimized (opto)electronic structures may be achieved by tuning the material properties through adjusting the composition of elements. This is only possible with a detailed understanding of the electronic band structure of the constituent materials and of their interfaces. Moreover, investigations of thin pseudomorphically grown strained heterostructures have introduced an additional degree of freedom in tailoring structural, electrical, and optical properties.[1,2]

Strained $In_xGa_{1-x}As/Al_yGa_{1-y}As$ quantum structures grown on GaAs are exemplary pseudomorphic systems with extremely well-suited properties for optical and electronic microdevices, e.g., index-guided lasers[3] and high-electron-mobility transistors.[4] Recently, considerable attention has been devoted to the band structure of strained $In_xGa_{1-x}As/GaAs$ heterointerfaces.[5–10] This system, similar to the unstrained $Al_yGa_{1-y}As/GaAs$ system, is a classic mix of the two binary compounds, InAs and GaAs. Extensive theoretical[5,6] and experimental[7–10] investigations have presented results for the band-energy discontinuities with some, though moderate, agreement.[7] For low alloy compositions (i.e., $x<0.30$ in $In_xGa_{1-x}As/GaAs$), where nonlinear variations in the conduction- and valence-band energies induced by material-dependent strain-related band shifts and ternary band-gap parabolicity are relatively small, the body of results indicates a constant conduction-band-offset ratio $\Delta Q_{cb}=\Delta E_{cb}/\Delta E_{gap}$, where ΔE_{cb} is the difference in conduction-band minima (in eV), and ΔE_{gap} is the difference in band gaps of the two materials.[10] However, it has recently been pointed out, particularly for strained quantum structures, that it is unreasonable to expect that ΔQ_{cb} will be constant over the entire composition range[11] owing to energy-gap parabolicity and strain-induced band-energy shifts that have nonlinear composition dependence.

Thus, while striving to achieve more advanced structures incorporating the greater band-gap difference between $Al_yGa_{1-y}As$ barrier material and strained $In_xGa_{1-x}As$ quantum structures, the nature of the interface alters drastically from the simple mix of two binary constituents to the relatively unexplored region of three binary compounds where two independent bowing factors and strain influence the band lineup. In the present paper the issue of band offsets at strained $In_xGa_{1-x}As/Al_yGa_{1-y}As$ interfaces pseudomorphically grown on GaAs is addressed from a theoretical point of view and compared to recent experimental data. In Sec. II the theoretical formalism based on the virtual-crystal approximation, or, correspondingly, linear-response theory (LRT),[12] is outlined and strain is introduced as a perturbative effect in a generalized theory of (100) interfaces. Section III introduces various concepts for the partitioning of the hydrostatic-strain component between the conduction and valence bands. A comparison of the calculated band-offset ratios using the different partitioning formulas is presented in Sec. IV, and the calculations are compared to recent experimental data. Conclusions are presented in Sec. V and further issues related to the nature of band discontinuities at strained ternary-ternary interfaces are discussed.

II. THEORETICAL FORMALISM

The starting point for the present formalism begins with adequate knowledge of the binary constituents. Most recently published values have been adopted for this work and are summarized in Table I. Where

discrepancies have been found in the literature (e.g., deformation potentials for InAs), calculations were performed over the range of values and the results were compared. Only minor variations of the calculated band discontinuities were observed, and the constants most recently reported in the literature were adopted as listed in Table I. All parameters related to the strain response of the system were linearly interpolated between the binary compounds.

The band-offset values for GaAs/AlAs and unstrained InAs/GaAs have been recently published and are given in Table I. Though some discrepancy exists over ΔE_{VB} for the InAs/GaAs interface, we have adopted the average value ($\Delta E_{VB}=0.17\pm0.07$ eV) found in a large number of publications.[7] Adequate knowledge of the valence-band offset for InAs/AlAs is more problematical due to the lack of experimental results and theoretical calculations for this specific interface (strained or unstrained). Consequently, we have adapted two methods to estimate this value. First, the transitivity rule[13] was applied to the values quoted in Table I and those recently compiled in Ref. 5, resulting in $\Delta E_{VB}=0.71\pm0.1$ eV for the unstrained InAs/AlAs interface. Correspondingly, results from investigations on lattice-matched $In_{0.53}Ga_{0.47}As/In_{0.52}Al_{0.48}As$ heterostructures[14,15] are extrapolated to yield a valence-band offset of $\Delta E_{VB}=0.75\pm0.04$ eV for the binary interface, in general agreement with the value predicted by the model solid theory ($\Delta E_{VB}=0.78\pm0.2$ eV) in Ref. 6. The average value of these results is reflected in Table I with a relatively high error of ±0.2 eV and represents the most unreliable data on which the calculations are based.

The general valence-band interface at $\mathbf{k}=\mathbf{0}$ is depicted in Fig. 1. The quantity of interest, ΔE_{VB} (or correspondingly, ΔE_{CB}, ΔQ_{CB}, and ΔQ_{VB}, where $\Delta E_{CB}+\Delta E_{VB}=\Delta E_{gap}$ and $\Delta Q_{VB}=\Delta E_{VB}/\Delta E_{gap}$) for a ternary-ternary interface is derived from knowledge of the unstrained binary interfaces (i.e., InAs/GaAs, InAs/AlAs, and GaAs/AlAs) and the behavior of the band gaps and spin-orbit band ($E_0+\Delta_0$) with composition and strain.

The unstrained nonrelativistic valence-band offset $\Delta E_{VB,nr}$ for the binary interfaces is then calculated as[6,12]

$$\Delta E_{VB,nr}=\Delta E_{VB}+\tfrac{1}{3}\Delta_0^{I}-\tfrac{1}{3}\Delta_0^{II}\ , \tag{1}$$

where ΔE_{VB} is given in Table I and the Δ_0's are the corresponding energies of the spin-orbit bands in semiconductors I and II (see Fig. 1). Considering the mixed ternary interface in the virtual-crystal approximation, the unstrained $In_xGa_{1-x}As/Al_yGa_{1-y}As$ valence-band offset is then[6,12,16]

TABLE I. Material parameters used in the calculations. All values are listed for 2 K. Values are from Ref. 11 and references therein unless otherwise noted.

Parameter (units)	GaAs	InAs	AlAs
E_g(2 K) (eV)	1.519	0.416	3.099[a]
Δ_0 (eV)	0.34	0.37	0.28[b]
a_0 (Å)	5.6536	6.059	5.6611[b]
C_{11} (10^{11} dyn/cm^2)	12.11	8.54	
C_{12} (10^{11} dyn/cm^2)	5.48	4.66	
a_c (eV)	−7.1	−5.4	
b_v (eV)	−1.7	−1.8	
dE_g/dp (10^{-6} eV cm^2/kg)	11.3	9.8	
$d(E+\Delta_0)/dP$ (10^{-6} eV cm^2/kg)	1.27[b]	1.08[b]	
ΔE_{VB} relative to GaAs (eV)		0.16[c]	0.57[d]
ΔE_{VB} relative to InAs (eV)		0.73[e]	
$E_{g,Al_yGa_{1-y}As}(y)$ (eV)	$1.519+1.36y+0.22y^2$ [a]		
$\Delta_{0,Al_yGa_{1-y}As}(y)$(eV)	$0.341-0.281y+0.22y^2$ [a]		
$E_{g,In_xGa_{1-x}As}(x)$ (eV)	$1.519-1.603x+0.50x^2$ [f]		
$\Delta_{0,In_xGa_{1-x}As}(x)$ (eV)	$0.341-0.101x+0.14x^2$ [g]		

[a]C. Basio, J. L. Staehli, M. Guzzi, G. Burri, and R. A. Logan, Phys. Rev. B **38**, 3263 (1988).
[b]*Semiconductors*, Vol. 17a of *Landolt-Börnstein, Functional Relationships in Science and Technology*, New Series, edited by O. Madelung, M. Schulz, and H. Weiss (Springer-Verlag, Berlin, 1982), Gp. 3.
[c]Reference 7, and references therein.
[d]Reference 5.
[e]Calculated using the transitivity rule from values in Refs. 5 and 6 and extrapolating the latticed-matched valence-band offsets reported in Refs. 14 and 15 to the binary constituents.
[f]K. H. Goetz, D. Bimberg, H. Jur, J. Selders, A. V. Solomonov, G. F. Glinskii, M. Razeghi, and J. J. Robin, J. Appl. Phys. **54**, 4543 (1983).
[g]O. Berolo and J. C. Wooley, in *Proceedings of the 11th International Conference on the Physics of Semiconductors, Warsaw, 1972* (Polish Scientific, Warsaw, 1972), p. 1420.

$$\Delta E_{\mathrm{VB,unstrained}} = x[y\Delta E_{\mathrm{VB,nr}}(\mathrm{InAs/AlAs}) + (1-y)\Delta E_{\mathrm{VB,nr}}(\mathrm{InAs/GaAs})] + (1-x)[y\ \Delta E_{\mathrm{VB,nr}}(\mathrm{AlAs/GaAs})] + \tfrac{1}{3}\Delta_0(x)(\mathrm{In}_x\mathrm{Ga}_{1-x}\mathrm{As}) - \tfrac{1}{3}\Delta_0(y)(\mathrm{Al}_y\mathrm{Ga}_{1-y}\mathrm{As}) + 3x(1-x)(\Delta a_v)\frac{\Delta a_0}{a_0(x)}\ , \tag{2}$$

where the last term is due to strain correction when considering the alloy as a superposition of atoms in the virtual crystal,[16] $\Delta a_v = a_v(\mathrm{GaAs}) - a_v(\mathrm{InAs})$, $a_v = dE/dP - a_c$, $\Delta a_0 = a_0(\mathrm{InAs}) - a_0(\mathrm{GaAs})$, $a_0(x) = xa_0(\mathrm{InAs}) + (1-x)a_0(\mathrm{GaAs})$, a_0 is the lattice constant, and the Δ's contain the appropriate bowing factors.

Strain is calculated according to our recent work[7] and is summarized below. For thin $In_xGa_{1-x}As$ layers pseudomorphically grown to $Al_yGa_{1-y}As$, we assume that all the strain is incorporated in the $In_xGa_{1-x}As$. For growth in the [001] direction, the $In_xGa_{1-x}As$ layer is thus biaxially compressed in the [100] and [010] directions and exhibits a corresponding expansion along the (001) plane. The strain ε of the sandwiched $In_xGa_{1-x}As$ layer is defined as

$$\varepsilon = \frac{a_{\mathrm{In}_x\mathrm{Ga}_{1-x}\mathrm{As}} - a_{\mathrm{Al}_y\mathrm{Ga}_{1-y}\mathrm{As}}}{a_{\mathrm{Al}_y\mathrm{Ga}_{1-y}\mathrm{As}}}\ , \tag{3}$$

where a represents the lattice constant. Pollak and Cardona[17] have developed an accurate description of the valence-band manifolds under strain which is given by the 6×6 Hamiltonian:

$$\mathcal{H}_{\mathrm{strain}} = -a(\varepsilon_{xx}+\varepsilon_{yy}+\varepsilon_{zz}) - 3b[(L_x^2 - \tfrac{1}{3}L^2)\varepsilon_{xx} + \mathrm{c.p.}] - \sqrt{3}d[(L_xL_y + L_yL_x)\varepsilon_{xy} + \mathrm{c.p.}]\ , \tag{4}$$

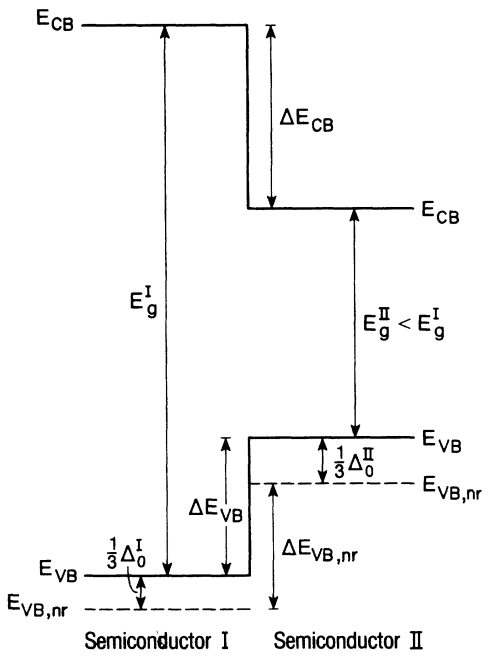

FIG. 1. Energy-band diagram at $\mathbf{k}=0$ for a generic type-I unstrained heterointerface between semiconductors I and II, where E_{VB} represents the top of the degenerate Γ_8 valence bands and Δ_0 is the spin-orbit band. ΔE_{VB} is the energy difference in the valence-band maxima, whereas $\Delta E_{\mathrm{VB,nr}}$ is the difference between the nonrelativistic valence-band maxima, where $E_{\mathrm{VB,nr}} = E_{\mathrm{VB}} - \frac{1}{3}\Delta_0$ for each material. The conduction-band positions are found by adding the band-gap energies to the respective valence-band maxima, and the conduction-band discontinuity ΔE_{CB} is calculated accordingly.

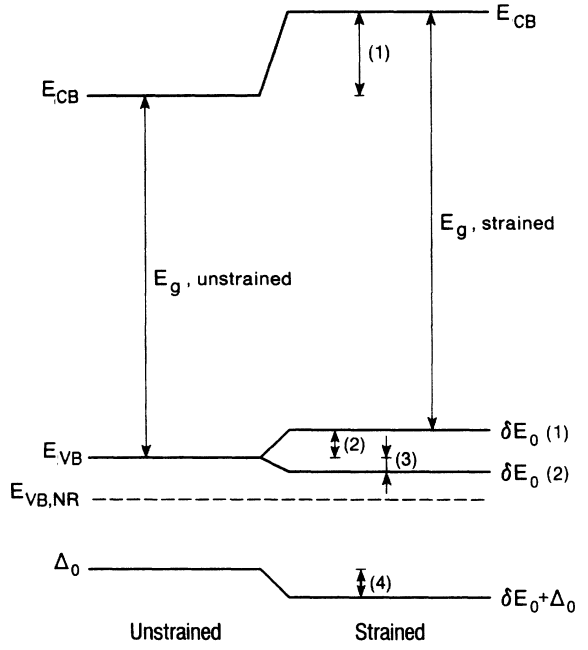

FIG. 2. Energy-band diagram outlining the influence of biaxial compressive strain and uniaxial tension on the band positions. E_{VB} is the top of the degenerate Γ_8 valence bands, $E_{\mathrm{VB,nr}}$ is the nonrelativistic or average valence-band position, and Δ_0 is the spin-orbit band. $\delta E_0(1)$ and $\delta E_0(2)$ are the now spin-split nondegenerate valence bands and $\delta E_0 + \Delta_0$ the spin-split spin-orbit band. $\delta E_0(2)$ can lie below or above the unstrained valence-band level, depending on the amount of strain (indium concentration) and the unstrained valence-band discontinuity (i.e., aluminum concentration). The conduction-band minima shift by an amount (1) given by $(1\text{-}\Delta Q_H)E_H$. $\delta E_0(1)$, $\delta E_0(2)$, and $\delta E_0 + \Delta_0$ shift by the amounts (2), (3), and (4) given by Eqs. (6a), (6b), and (6c), respectively. $E_{\mathrm{VB,nr}}$ is relatively insensitive to strain and is thus shown not to vary.

where ε_{ij} are the components of the strain tensor, L is the angular-momentum operator, and c.p. denotes cyclic permutation with respect to the axes x, y, and z. The quantities a, b, and d are deformation potentials under hydrostatic, tetragonal, and trigonal perturbation, respectively. For growth in the [001] direction,

$$\varepsilon_{xx}=\varepsilon_{yy}=\varepsilon,\ \varepsilon_{zz}=-K\varepsilon\ ,$$
$$\varepsilon_{xy}=\varepsilon_{yz}=\varepsilon_{xz}=0\ . \tag{5}$$

Diagonalization of the reduced Hamiltonian yields three eigenvalues at $\mathbf{k}=\mathbf{0}$ with the corresponding energy shifts given by

$$\delta E_0(1)=E_H+E_S\ , \tag{6a}$$

$$\delta E_0(2)=E_H-\tfrac{1}{2}\Delta_0-\tfrac{1}{2}E_S+\tfrac{1}{2}(\Delta_0^2+2\Delta_0E_S+9E_S^2)^{1/2}\ , \tag{6b}$$

$$\delta E_0+\Delta_0=E_H-\tfrac{1}{2}\Delta_0-\tfrac{1}{2}E_S-\tfrac{1}{2}(\Delta_0^2+2\Delta_0E_S+9E_S^2)^{1/2}\ , \tag{6c}$$

with $E_H=a(2-K)\varepsilon$, $E_S=b(1+K)\varepsilon$, and $K=-2S_{12}/(S_{11}+S_{12})$, where S_{ij} are the standard elasticity relations. The strain-shifted energy bands labeled $\delta E_0(1)$ and $\delta E_0(2)$ denote the now spin-split nondegenerate Γ_8 valence-band components, and $\delta E_0+\Delta_0$ the spin-split spin-off band. Under compressive stress, $\delta E_0(1)$ and $\delta E_0(2)$ correspond to the heavy- and light-hole valence bands, respectively. The influence of compressive biaxial strain and uniaxial stress on the energy bands at $\mathbf{k}=\mathbf{0}$ are displayed schematically in Fig. 2. The biaxial hydrostatic strain influences both the conduction band [by a relative amount $(1-\Delta Q_H)E_H$] and the valence bands (by $\Delta Q_H E_H$) with an overall effect which increases the band gap. Uniaxial tension further influences the valence bands, effectively decreasing the band gap and inducing mixing of the $|\frac{3}{2},\frac{1}{2}\rangle$ and $|\frac{1}{2},\frac{1}{2}\rangle$ bands.[17]

III. PARTITIONING OF THE HYDROSTATIC-STRAIN COMPONENT

Partitioning of the hydrostatic-strain-induced band shifts, as previously mentioned, is proportional to the relative sensitivity of the band manifolds in relation to the changes in the band gap with pressure. In our earlier paper, which concentrated on the band offsets at the strained $In_xGa_{1-x}As/GaAs$ interface,[7] a partitioning coefficient ΔQ_H, defined as the ratio of the spin-orbit band deformation potential to the total change in the band gap under pressure, or

$$\Delta Q_{H1}=\left[\frac{d(E_g+\Delta_0)}{dP}(x)\right]\left[\frac{dE_g}{dP}(x)\right]^{-1}\ , \tag{7}$$

was proposed as an appropriate measure of the valence-band sensitivity to hydrostatic pressure, relative to the total change in band gap. In the present investigation, this parameter is allowed to vary as a function of composition, in agreement with the linearized material parameters used, and is represented by ΔQ_{H1}. More recently, Gershoni *et al.* have used a ternary band-gap hydrostatic deformation potential,[11] given in the large square brackets of Eq. (8), from which we may define a partitioning coefficient ΔQ_{H2} as

$$\Delta Q_{H2}=1-\left[\frac{a_c(x)}{\left[\left[\frac{-dE_g}{dP}(x)\right]\frac{1}{3}[C_{11}(x)+2C_{12}(x)]\right]}\right]\ , \tag{8}$$

where $a_c(x)$ is the ternary conduction-band hydrostatic deformation potential and the $C_{ij}(x)$ are the ternary stiffness-coefficient tensor components.

Additionally, we define a third partitioning coefficient ΔQ_{H3} simply as

$$\Delta Q_{H3}=1-\left[a_c(x)\left[\frac{dE_g}{dP}(x)\right]^{-1}\right]\ , \tag{9}$$

which is equivalent to the expression developed for the hydrostatic deformation of the average valence band [Eq. (6) in Ref. 6].

IV. RESULTS

Figure 3 shows the variation of the strained (heavy-hole) valence-band discontinuity as a function of indium mole fraction x for various aluminum mole fractions y for a strained $In_xGa_{1-x}As/Al_yGa_{1-y}As$ heterointerface. The curves are calculated using the hydrostatic partitioning coefficient ΔQ_{H3}, and by considering the

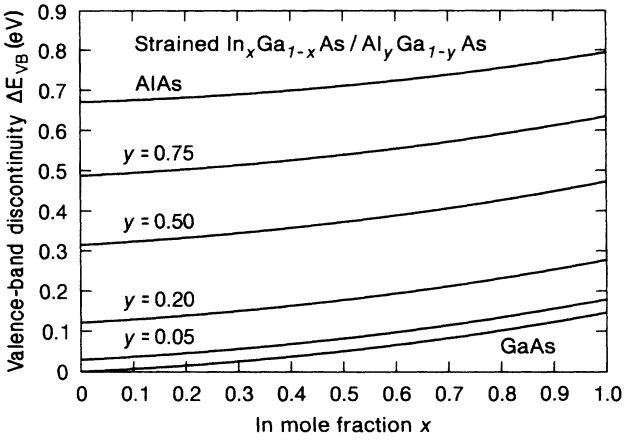

FIG. 3. Strained valence-band (heavy-hole) discontinuity ΔE_{VB} (eV) as a function of indium mole fraction x, presented for different aluminum compositions y for $In_xGa_{1-x}As/Al_yGa_{1-y}As$ interfaces. Values have been calculated using the hydrostatic partitioning coefficient ΔQ_{H3} defined in Eq. (9). The observed nonlinear behavior results from including band parabolicity and nonlinear strain-dependent band deformations. The energy separation among the different curves is approximately equal to the increase in band gap of the $Al_yGa_{1-y}As$ at higher y.

$GaAs/Al_yGa_{1-y}As$ component as a constant percentage of the band-gap difference, consistent with the majority of observations[5] that, at low y, ΔE_{VB} for $GaAs/Al_yGa_{1-y}As$ varies linearly with y. The observed spacing between two curves is approximately the difference in band gap of the $Al_yGa_{1-y}As$ for the corresponding Al contents y. For Al content $y > 0.4$ (indirect region), the Γ conduction-band minimum was chosen as the reference level. Relative to the unstrained band discontinuity, the valence-band maxima rise to ~ 0.15 eV, whereas the total shift in the band gap can be as great as 0.37 eV. The corresponding valence-band-offset ratios ΔQ_{VB} vary from 0.15 to greater than 0.40 for InAs/GaAs and from 0.10 to 0.25 for $InAs/Al_{0.3}Ga_{0.7}As$.

Furthermore, the band-offset ratios are found to vary widely as a function of indium composition, as shown for the conduction-band-offset ratio ΔQ_{CB} in Fig. 4. Here, the strained conduction-band ratio ΔQ_{CB} is plotted as a function of indium mole fraction x for a given aluminum content $y=0.2$. Curves (a), (b), and (c) are calculated according to the hydrostatic partitioning coefficients ΔQ_{H3}, ΔQ_{H2}, and ΔQ_{H1}, respectively. For comparison, the only experimental data available (solid dots),[18] to our knowledge, are also plotted. Within the accuracy of the experimental findings, which are reported with errors of $\pm$ (10–15) meV,[18] it is quite clear from the comparison between the calculated and experimental values that ΔQ_{H3} is the most appropriate formalism to calculate the amount of hydrostatic deformation occurring in the valence bands. Additionally, the extrapolated strained valence-band offset for InAs/AlAs is found to be 0.77 eV, in good agreement with the experimental findings of Moisin *et al.*,[19] who report $\Delta E_{VB}=0.72\pm0.07$ eV, and with the value of 0.95 ± 0.2 eV predicted by the model solid theory.[6] The experimental ΔQ_{CB} of Ref. 18 are reported to follow a linear dependence on x. This is most probably an artifact arising from the limited composition region investigated. Extrapolation of these values to high indium content would lead to ΔQ_{CB} greater than 1, contrary to previous experimental findings [19] and theoretical predictions.[6] More appropriately, when material parameters are treated as composition dependent, and the unstrained valence-band discontinuities are calculated within the virtual-crystal approximation, the band-offset ratios are found to saturate as x increases for the case of ΔQ_{H3} or reach a maximum and then decline for the cases of ΔQ_{H1} and ΔQ_{H2}.

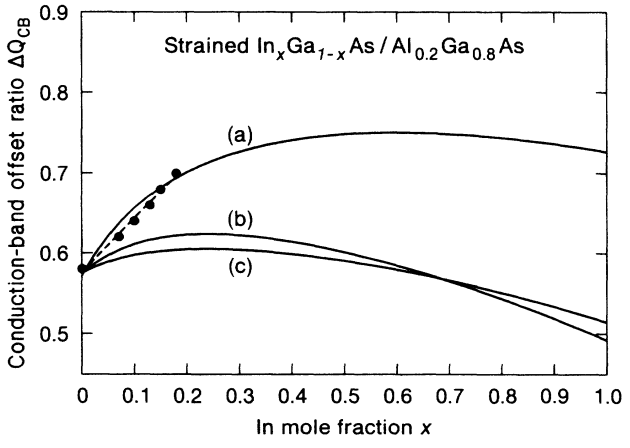

FIG. 4. Strained conduction-band-offset ratio ΔQ_{CB} as a function of indium mole fraction x for $In_xGa_{1-x}As/Al_{0.2}Ga_{0.8}As$ interfaces calculated with the three different hydrostatic partitioning coefficients: (a) ΔQ_{H3}, (b) ΔQ_{H2}, and (c) ΔQ_{H1}. Recent experimental data from Ref. 18 (●) and the corresponding least-squares fit (dashed line) are also shown.

In comparison to curve (a) of Fig. 4, the behavior of ΔQ_{CB} when calculated with ΔQ_{H1} and ΔQ_{H2} is qualitatively similar, though distinctly different in absolute variation. The ΔQ_{CB} calculated using ΔQ_{H3} is dramatically higher since the hydrostatic deformation induces a downward shift of the valence-band manifolds, thus reducing the effective potential height of the valence-band discontinuity. The greater hydrostatic deformation of the valence band is due to a larger partitioning coefficient. ΔQ_{H3} is found to vary between 0.37 and 0.45 with increasing x and is 3–4 times greater than the corresponding values of ΔQ_{H1} and ΔQ_{H2}. The behavior at higher x reflects the relative difference between the hydrostatic- and uniaxial-strain contributions to the (heavy-hole) valence-band movement. At higher strain values, the stress-related elongation along the growth direction induces almost equivalent, or sometimes greater, band shifts than the hydrostatic deformation. This, in turn, increases the effective valence-band discontinuity or, equivalently, decreases ΔQ_{CB}.

Within the general theoretical framework of Sec. II, and the comparisons presented specifically for the strained $In_xGa_{1-x}As/Al_yGa_{1-y}As$ interface above, the sensitivity of the Γ_8 valence bands to pressure is most accurately described by the simple difference between the band gap and conduction-band deformation potentials without additional stiffness tensor factors. The composition-dependent stiffness tensor components are fully accounted for in Eqs. (3–6), and, in fact, when reintroduced, as in Eq. (8), underestimate the hydrostatic-pressure-induced change of the Γ_8 valence band. Additionally, the deformation of the Γ_8 bands is not equivalent to that of the spin-orbit band ($E_0+\Delta_0$), as can be appreciated by comparing curves (a) and (b) in Fig. 4. It is worth noting that the theory developed in Sec. II is general and may be applied to any heterointerface with similar symmetry properties.

Figure 5 shows the variation of the strained conduction-band-offset ratio ΔQ_{CB} as a function of indium mole fraction x for various aluminum contents y. Recall that for $y > 0.4$ the conduction band of the strained $In_xGa_{1-x}As$ is referenced to the now higher-lying Γ band of the $Al_yGa_{1-y}As$. The striking nonconstant behavior of the $y=0.05$ curve is somewhat surprising and is currently under investigation.[20] In general, however, ΔQ_{CB} displays distinctly nonconstant behavior as a function of x, in agreement with earlier predictions,[11] and is extremely variable at low y values and becomes more

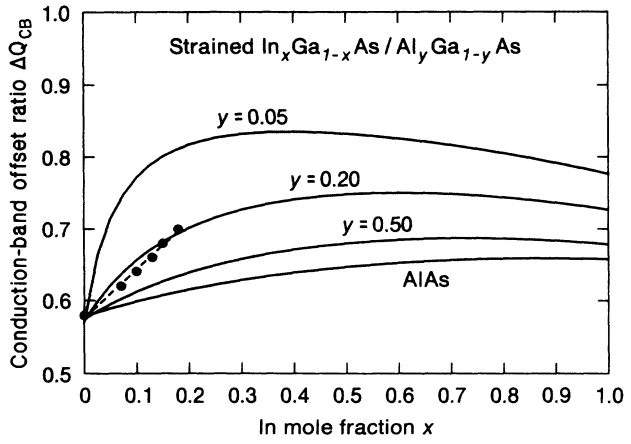

FIG. 5. Strained conduction-band-offset ratio ΔQ_{CB} as a function of indium mole fraction x for $In_xGa_{1-x}As/Al_yGa_{1-y}As$ interfaces calculated with ΔQ_{H3} and compared to recent experimental data (●) for $y=0.2$ (Ref. 18) and the corresponding least-squares fit (dashed line).

linear as y increases. Of particular interest for heterointerfaces, where the band discontinuity plays a crucial role in carrier confinement, is that increasing the Al content gives the added benefit of increased differences in the band gaps of the materials, but only at the expense of a reduction in the conduction-band-offset ratio. This could be of significant importance in the design of strained-layer, high-electron-mobility transistors and quantum-well lasers where the band discontinuities directly influence carrier confinement and device performance.

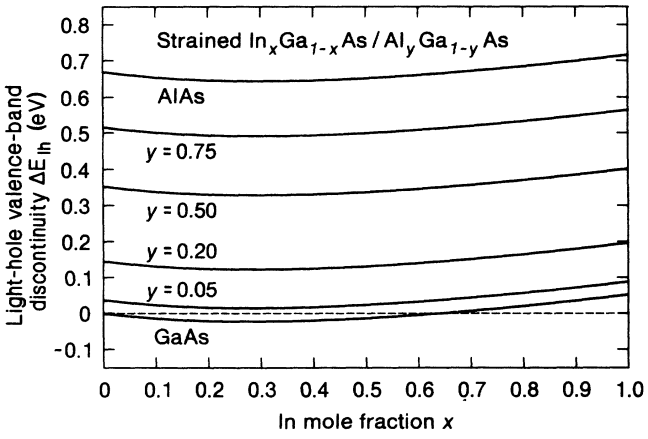

FIG. 6. Strained light-hole valence-band discontinuity ΔE_{lh} as a function of indium mole fraction x for $In_xGa_{1-x}As/Al_yGa_{1-y}As$ interfaces calculated with ΔQ_{H3} and presented for various aluminum contents y. The data lying under the dashed horizontal line at $\Delta E_{lh}=0$ indicate that the light-hole band will be confined in the barrier valence bands, and result in a type-II heterostructure for electron–light-hole transitions.

Owing to the stress-induced splitting of the highest-lying valence bands, the light-hole band lies lower than the heavy-hole band for compressive biaxial strain and uniaxial tension. Thus, under proper conditions, the light-hole band may reside below the valence-band maxima of the barrier material, e.g., a type-II heterostructure. This case is well known for a number of semiconductors[21] and has recently been shown to be also possible in strained $In_xGa_{1-x}As/GaAs$ quantum wells and superlattices.[2] Figure 6 shows the corresponding strained light-hole valence-band discontinuity ΔE_{lh} plotted as a function of indium mole fraction x and aluminum content y. The dashed horizontal line at $\Delta E_{lh}=0$ indicates the transition from type-I to type-II interfaces. When $\Delta E_{lh}<0$, the light-hole band resides in the barrier valence band, resulting in a type-II interface. This case is only possible for strained $In_xGa_{1-x}As/GaAs$ (e.g., $y=0$) structures with $x<\sim 0.60$. With increasing Al content, the strain-induced band changes are smaller than the unstrained valence-band discontinuity which increases with y, prohibiting the formation of a type-II interface. The extreme nonlinear behavior of ΔE_{lh} follows from the spin-splitting interaction described by Eq. (6b).

V. CONCLUSIONS

The band-edge discontinuities of strained $In_xGa_{1-x}As/Al_yGa_{1-y}As$ heterointerfaces have been calculated within the virtual-crystal approximation as a function of indium and aluminum content, accounting for band parabolicity and incorporating composition-dependent material parameters. Three formalisms for the partitioning of the hydrostatic-pressure-induced band shifts between the conduction and valence bands were investigated and calculated results were compared to recent experimental data. Our results indicate that the pressure sensitivity of the Γ_8 valence bands is simply the difference between the pressure sensitivity of the band gap and the conduction-band deformation potential, without additional modification by ternary stiffness components, and that more than 30% of the hydrostatic band-gap deformation affects the valence bands for strained $In_xGa_{1-x}As$. The strained band-offset ratios are found to be variable and nonlinear over the entire composition range and vary dramatically with aluminum content. Type-II heterostructures formed with the strained spin-split light-hole valence band are found to be possible, but only in the case of $In_xGa_{1-x}As/GaAs$ heterostructures with indium content $x<\sim 0.60$. Our findings suggest that the incorporation of strain in ternary-ternary heterostructures adds a new dimension to achieving desired electronic band structure and new quantum devices.

ACKNOWLEDGMENTS

Helpful discussions with W. von der Linden, G. Borghs, A. Baldereschi, and Y. Galeuchet, and the support of the Laser Science and Technology Department, are gratefully acknowledged.

[1]G. C. Osbourn, Phys. Rev. B **27**, 5126 (1989).
[2]J. Y. Marzin, M. M. Charasse, and B. Sermage, Phys. Rev. B **31**, 8298 (1985).
[3]R. M. Kolbas, N. G. Anderson, W. D. Laidig, Y. Sin, Y. C. Lo, K. Y. Hsieh, and Y. J. Yang, IEEE J. Quantum Electron. **QE-24**, 1605 (1988).
[4]G. I. Ng, W. Hong, D. Pavldis, M. Tutt, and P. K. Bhattacharya, IEEE Electron Dev. Lett. **EDL-9**, 439 (1988).
[5]J. M. Langer, C. Delerue, M. Lannoo, and H. Heinrich, Phys. Rev. B **38**, 7723 (1988).
[6]C. G. Van De Walle, Phys. Rev. B **39**, 1871 (1989), and references therein.
[7]D. J. Arent, K. Deneffe, C. Van Hoof, J. De Boeck, and G. Borghs, J. Appl. Phys. **66**, 1739 (1989).
[8]F. Iikawa, F. Cerdeira, C. Vazquez-Lopez, P. Motisuke, M. A. Sacilotti, A. P. Roth, and R. A. Masut, Phys. Rev. B **38**, 8473 (1988).
[9]S. H. Pan, H. Shen, Z. Hang, F. H. Pollak, W. Zhuang, Q. Xu, A. P. Roth, R. A. Masut, C. Laselle, and D. Morris, Phys. Rev. B **38**, 3375 (1988).
[10]S. Niki, C. L. Lin, W. S. C. Chang, and H. H. Wieder, Appl. Phys. Lett. **55**, 1339 (1989).
[11]D. Gershoni, J. M. Vandenberg, S. N. G. Chu, T. Tanbun-Ek, and R. A. Logan, Phys. Rev. B **40**, 10017 (1989).
[12]R. Resta, S. Baroni, and A. Baldereschi, Superlatt. Microstruct. **6**, 31 (1989).
[13]N. E. Christensen, Phys. Rev. B **38**, 12687 (1988), and references therein.
[14]R. People, K. W. Wecht, K. Alavi, and A. Y. Cho, Appl. Phys. Lett. **43**, 118 (1983).
[15]A. Sandhu, Y. Nakata, S. Sas, K. Kodama, and S. Hiyamizu, Jpn. J. Appl. Phys. Pt.1 **26**, 1709 (1987).
[16]M. Cardona and N. E. Christensen, Phys. Rev. B **37**, 1011 (1988).
[17]F. H. Pollak and M. Cardona, Phys. Rev. **172**, 816 (1968).
[18]N. Debbar, D. Biswas, and P. Bhattacharya, Phys. Rev. B **40**, 1058 (1989).
[19]J. M. Moisin, C. Guille, M. Van Rompay, F. Barthe, F. Houzay, and B. Bensoussan, Phys. Rev. B **39**, 1772 (1989).
[20]D. J. Arent, C. Van Hoof, G. Borghs, and H. P. Meier (unpublished).
[21]There are numerous well-known type-II interfaces, such as InAs/GaSb. The reader is referred to the review by L. Esaki, IEEE J. Quantum Electron. **QE-22**, 1611 (1986).